09

Laser-written waveguides in lithium niobate: fabrication and optical loss characterization during fiber coupling

© M.P. Smayev,[1] R.S. Ponomarev[2]

[1] Lebedev Physical Institute, Russian Academy of Sciences,
119991 Moscow, Russia
[2] Perm State University,
614068 Perm, Russia
e-mail: smayev@lebedev.ru

Received June 1, 2025
Revised November 26, 2025
Accepted November 29, 2025

Direct femtosecond writing of optical structures in the bulk material is an actively developing technique for fabricating integrated photonic elements, particularly attractive for nonlinear media, where tuning the recording beam parameters enables control over the frequency conversion of guided light. To create multifunctional photonic devices, waveguides inscribed in a crystal must be coupled to optical fibers, with minimized optical losses being essential for proper device integration. We investigated the regimes of laser modification of a lithium niobate single crystal using femtosecond pulses at a wavelength of 1030 nm, enabling the formation of polarization-sensitive tracks with a reduced refractive index. Waveguides with an unmodified $LiNbO_3$ core and a cladding consisting of 32 tracks with lower refractive index were fabricated via laser beam scanning. The coupling of optical fibers with the input and output facets of the crystal was implemented. The fabrication waveguides exhibited propagation losses as low as 2 dB/cm.

Keywords: direct laser writing, femtosecond pulses, channel waveguide, depressed cladding, lithium niobate, negative uniaxial crystals.

DOI: 10.61011/TP.2026.04.63274.134-25

Introduction

Lithium niobate $LiNbO_3$ is widely known for its electro-optical, acousto-optical, nonlinear optical characteristics [1,2]. Lithium niobate is a ferroelectric and $LiNbO_3$ exhibited a Pockels effect, photoelasticity and nonlinear optical polarizability and they were studied. It is characterized by a wide transparency band, high values of the Curie temperature ($T_c = 1210\,^\circ\mathrm{C}$), piezoelectric and electro-optical coefficients. An optical band gap of a lithium niobate single crystal is $E_g = 3.7\,\mathrm{eV}$. Due to its unique characteristics, this crystal has been given a large number of studies both in terms of investigating its fundamental properties as well as possible and implemented applications.

Writing of buried waveguide structures in media with pronounced nonlinear optical properties is a promising field, since it makes it possible to focus light emission energy in a controlled material volume. It is interesting for forming localized nonlinear devices for generating harmonics, self-modulation effects, generating summary and difference frequencies.

Uniqueness of the optical properties, primarily, high values of quadratic nonlinearity coefficients $\chi^{(2)}$ makes lithium niobate attractive for writing the waveguide structures therein. There are various methods known for forming the waveguides in the $LiNbO_3$ bulk: proton exchange [3–5], solid-state diffusion [6–8], ion implantation, femtosecond laser writing [9–12], etc.

Application of proton exchange or ion diffusion makes it possible to form two-dimensional waveguide structures. These approaches are applicable both for creating waveguides over the entire material surface as well as their formation in selected micro-regions. These process methods are complex, multi-staged and, therefore, quite expensive. In case of planar structures, ultrahigh requirements are also applied to a crystal surface quality, since it functions as an upper reflecting boundary of the waveguide. Besides, a composition, a structure and properties of a crystal subsurface layer significantly affect the process and a profile of a refractive index of the formed waveguides [13,14].

Writing of the optical waveguides in transparent dielectric materials by femtosecond laser pulses is an extensively developing technology and means modifying material properties by a moving focused beam of ultrashort pulses [15–19]. The femtosecond modification stands out against other procedures by a single-stage nature of a process of fabrication of photonic integrated circuit elements, which does not require a labor-intensive mask manufacturing process unlike traditional photolithography methods.

Depending on constitutive parameters of the medium and laser irradiation characteristics, the femtosecond impact can result both in an increase of the refractive index in the modified region ($\Delta n > 0$, the Type I modification) and its reduction as well ($\Delta n < 0$, Type II) [20,21]. A light-guiding core can be written both by single [22] and multiple scanning [20,23,24] of a selected region. In case

of modification when $\Delta n > 0$, it includes writing of the waveguide core, which is directly a light-guiding channel. In case of Type II modification, the waveguide shall be formed by writing of a cladding that consists of a set of channels (when $\Delta n < 0$) [25]. This waveguide structure has leaky modes propagating [26,27]. The channel waveguides with positive variation of the refractive index in the core ($\Delta n > 0$) are attractive due to relative writing simplicity, while the waveguides with a lower refractive index in the cladding are advantageous since the core is not affected, thereby making it possible to monitor waveguide characteristics of the unmodified region and to save a value of the electro-optical coefficients.

The parameters of light guiding by the written structures depend on many factors, which are both related to parameters of proper laser radiation (energy and duration of a pulse, a pulse repetition rate) as well as non-laser ones (a sample motion speed, focusing optics, a material and structure of the sample). Changing the lithium niobate structure and producing the channel waveguide by femtosecond modification (a wavelength $\lambda = 775\,\text{nm}$, duration $\tau_p = 150\,\text{fs}$, a repetition rate $\nu = 1\,\text{kHz}$, single-pulse energy $E_p = 10\,\mu\text{J}$, a scanning speed $V_{wr} = 50\,\mu\text{m/s}$) at the depth of $500\,\mu\text{m}$ under a polished surface of the sample is described in the study [9]. This study has observed the increase of the refractive index and written an Y-splitter. A cross-section of the channel waveguide was ellipsoidal and a maximum of contrast of the refractive index reached $6 \cdot 10^{-4}$. During propagation of the 633 nm-wavelength beam, losses were 1 dB/cm. However, despite successful demonstration of waveguide functioning, polarization properties of guided light were not studied. Fabrication of the two-dimensional and three-dimensional channel waveguide splitters in a $LiNbO_3$ Z-transect by direct femtosecond laser writing with an increase of the unusual wave's refractive index n_e with losses below 4 dB/cm is described in the study [28].

For forming polarization-sensitive waveguide structures in the $LiNbO_3$ *Z*-transect, the study [29] used radiation with the wavelength of 800 nm ($\tau_p = 520\,\text{fs}$, $\nu = 5\,\text{kHz}$) that was focused at the depth of $250\,\mu\text{m}$ by a lens with a numerical aperture NA = 0.4. The waveguides were written in single scanning along the *X* axis and various light guiding modes were obtained depending on the pulse energy. With the energy being 300–400 nJ, laser impact resulted in destruction of the material inside a focal region along the entire written channel. But it made it possible to fulfill guiding around the focal region as a result of density redistribution, wherein it guided light polarized both along the optical axis as well as perpendicular to it. With the smaller energies, the material was not destroyed and the written channels exhibited radiation guiding that in principle depends on polarization of passing light. Thus, the beam polarized along the optical axis (the *Z* axis) is quite well transferred, while the orthogonally-polarized one scatters in volume. The authors of the study [29] related polarization-dependent guiding to local amorphization, which results in formation of the channel with the refractive index that is intermediate between a minimum one corresponding to the unusual wave refractive index n_e and a maximum one corresponding to the usual wave refractive index n_o. This light polarized along the optical axis was „in a polarized way“ limited by a region with the smaller refractive index and, consequently, passed through the waveguide.

Writing a waveguide track in $LiNbO_3$ with ultrashort pulses ($\lambda = 800\,\text{nm}$, $\nu = 1\,\text{kHz}$, NA = 0.65) at the scanning speed of $100\,\mu\text{m/s}$ is described in the study [30]. At the same time, light guiding was obtained in the same track under femtosecond impact ($\tau_p = 220\,\text{fs}$) or in a track-adjacent region (with the lower refractive index) with higher light-induced refraction due to an increase of the density as a result of material redistribution (when $\tau_p = 1.1\,\text{ps}$). For both the cases, the increase of the refractive index is related to a change of a crystal structure of the sample. The study [31] has investigated writing of the waveguides ($\lambda = 800\,\text{nm}$, $\tau_p = 40\,\text{fs}$, $\nu = 1\,\text{kHz}$, NA = 0.65) in the *X*- and *Z*-transects of lithium niobate. With the pulse energy being below $E_p = 0.5\,\mu\text{J}$, the *Z*-transect exhibited thermally unstable waveguides that were highly-selective to polarization. In the *X*-transect samples, irradiation resulted in material damage and reduction of the refractive index in the focal volume. But for this case it is also possible to guide in the unmodified stress region around the written track.

Impact of the femtosecond pulses also made it possible to write the channel waveguides with the core ($\Delta n > 0$) in $LiNbO_3$ with multiple scanning (writing of several dozens of tracks with a transverse step of $0.4\,\mu\text{m}$). This purpose was attained by using the *Z*-transect of lithium niobate with a periodic domain structure and irradiation with $\lambda = 1030\,\text{nm}$, $\tau_p = 350\,\text{fs}$, $\nu = 600\,\text{kHz}$, NA = 0.65. It was noted that unlike usual single writing of the core this case included no degradation of the nonlinear optical properties of the material [23,24].

Formation of the depressed-cladding waveguides in $LiNbO_3$ has been quite extensively studied [11,12,32–38]. Thus, the study [32] has formed the waveguides of a diameter 50 and $110\,\mu\text{m}$ when using radiations with the wavelength of $\lambda = 800\,\text{nm}$ at duration $\tau_p = 350\,\text{fs}$ ($\nu = 1\,\text{kHz}$, NA = 0.4), which sustained guiding both of the unusual and the usual wave, wherein annealing of $LiNbO_3$ made it possible to significantly reduce the losses. The studies [12,33] have implemented a single-mode waveguide with a depressed cladding and a squared core.

It is important to note that tubular waveguides produced by direct writing are usually less sensitive to polarization of input light and naturally enable extensive control of a core shape, i.e. a shape of the transferred laser mode, including formation of adiabatic tapers designed to reduce optical losses when coupling a chip to an optical fiber [39–41].

The present study has determined optimal parameters of formation of the waveguides with the depressed cladding in the *X*-transect of single-crystal lithium niobate by femtosecond pulses with the wavelength of 1030 nm depending on

polarization of writing radiation and determined parameters of guiding of laser radiation when coupling the optical fiber to sample butt ends to the waveguide formed by the femtosecond pulses.

1. Sample and unit for laser modification

An original sample was a $LiNbO_3$ X-transect crystal with a congruous composition (48.6 mol.% Li_2O) that was cut out of a plate manufactured by Crystal Technology. The sample was shaped as a parallelepiped of the size $15 \times 10 \times 1$ mm with polished facets. In order to create tracks of a modified refractive index, a light beam was focused in the crystal volume and then it was written by moving a table with the sample relative to the fixed beam. In an experiment performed, the channels of the modified refractive index were formed along the optical axis of the crystal. Lithium niobate is a negative uniaxial crystal. The refractive indices for the usual and the unusual wave at the wavelength of $\lambda = 1030$ nm are $n_o = 2.23$ and $n_e = 2.16$.

The $LiNbO_3$ crystal was modified by laser using a femtosecond oscillator with a regeneration amplifier based on the Yb:KGW crystal, which radiates at the wavelength of $\lambda = 1030$ nm. Pulse duration was $\tau_p = 175$ fs and the pulse repetition rate could vary within the range $\nu = 1$ kHz-1 MHz. The sample was installed onto an air-cushioned translational table (Fig. 1) designed to position the sample at a low vibration level with high precision. The light beam was focused in the $LiNbO_3$ volume by means of the Olympus LCPlanN 50$\times$ lens having the numerical aperture NA = 0.65. Polarization of the light beam was linear and its direction could be controlled by means of a motorized half-wave plate. The modification process was visualized on-line by means of a CCD camera and light-emitting diode illumination.

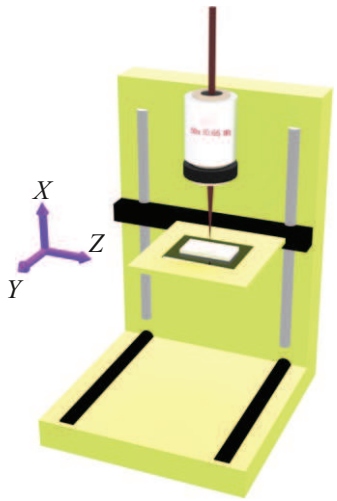

Figure 1. Diagram of femtosecond modification of $LiNbO_3$: the light beam ($\lambda = 1030$ nm) was focused in the volume of the moving crystal by means of the lens with the numerical aperture NA = 0.65. When the tracks were written, the sample was scanned along the Z axis that coincides with the optical axis of single-crystal $LiNbO_3$.

The regions of modification were primarily analyzed by means of the Olympus BX-61 optical microscope equipped with a vertically-motorized sample stage and a 14-bit camera. Recording a z-stack (the set of photos of a phase object) was followed by determining contrast of the refractive index Δn in the written tracks as compared to a surrounding unmodified region by Quantitative Phase Microscopy (QPM) [42–44].

2. Writing of the tracks of the lower refractive index

2.1. Determination of the modification threshold

Conditions of femtosecond modification greatly vary for the various laser systems and largely depend on characteristics of a specific sample. In this regard, optimal writing parameters were searched. The moving sample was irradiated by a beam of the femtosecond pulses with the repetition rate $\nu = 15$ kHz. The beam was buried under the surface of the polished sample at a distance of about $H = 65\,\mu$m and it was scanned along the optical axis of the crystal (the Z axis) at the speed $V_{wr} = 0.5$ mm/s. The threshold of femtosecond modification was determined for two orthogonal polarizations of the light beam relative to the scanning direction (Fig. 2, *a*). A polarization plane could be directed either along the scanning direction (wherein it is written by the unusual wave) or perpendicular to the scanning direction (in this case it is written by the usual wave).

It was written at the various femtosecond-pulse energies E_p. It was found that the modification threshold $E_p = 20$ nJ for both the polarizations. In the range 20$-$220 nJ, we have obtained smooth tracks (Fig. 2, *a*), which are vertically elongated (Fig. 2, *b*). The profile of the written tracks was analyzed from the butt end to show that the tracks formed by the usual light wave ($\mathbf{E} \perp \mathbf{V}_{wr}$) are somewhat below the tracks written by the unusual light wave ($\mathbf{E} \parallel \mathbf{V}_{wr}$) (by 3 μm when $E_p = 220$ nJ, Fig. 2, *b*), which is explained by the high refractive index n_o for the usual wave.

In all the tracks, variation of the refractive index was negative as compared to the unmodified region, which can be explained by reduction of a crystallinity degree of the modified region. The respective dependence of light-induced variation of the refractive index on the writing beam pulse energy is shown in Fig. 2, *c*. The tracks formed by the usual light wave are characterized by large contrast of the refractive index when the writing pulse energies $E_p > 50$ nJ. When the energy increases from 20 to 220 nJ, the track height increases from 5 to 12 μm (Fig. 2, *c*).

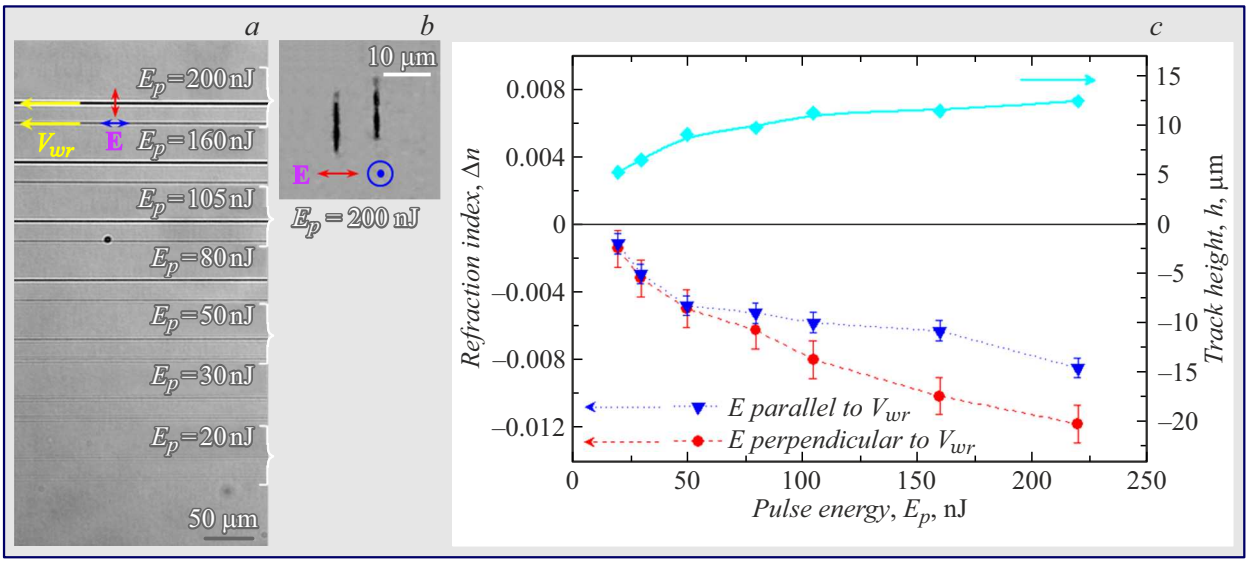

Figure 2. Series of the tracks of the modified refractive index, which are written in the $LiNbO_3$ crystal by femtosecond pulses ($\tau_p = 175$ fs, $\nu = 15$ kHz) with the various energy. E is a direction of polarization of the writing beam. The scanning speed $V_{wr} = 0.5$ mm/s. The images are obtained by means of an optical microscope: a — a plan view; b — a view from the butt end to the tracks formed with pulse energy $E_p = 200$ nJ; c — dependences of a track height h and variation of the refractive index Δn on the laser pulse energy for the two directions of polarization.

2.2. Variation of the pulse repetition rate and the scanning speed

In order to create homogeneous tracks by the scanning beam of ultrashort pulses, it is necessary to maintain a constant number of the pulses N_p hitting the sample, which is determined by the relationship [17,45]:

$$N_p = \frac{D \cdot \nu}{V_{wr}}, \qquad (1)$$

where D is a laser spot diameter. Depending on the light-pulse repetition rate ν, various modes of femtosecond modification are possible, while the speed variation range is quite narrow — when V_{wr} is low multi-track waveguides will be written exceedingly long, and when V_{wr} is high, limitations will appear due to a translational system (vibrations, inhomogeneities of acceleration and deceleration when a scanning path is short). Therefore, in order to search for an optimal writing mode that makes it possible to create the smooth tracks with maximum contrast of the refractive index Δn, $LiNbO_3$ was modified with proportional variation of the pulse repetition rate ν and the beam scanning speed V_{wr}. With the constant value of the number of the pulses N_p, for each pair ν and V_{wr} we have formed the tracks at the constant energy $E_p = 80$ nJ within the femtosecond pulse for the two orthogonal polarizations of writing radiation (Fig. 3). The tracks written by the usual light wave (with polarization orthogonal to the scanning direction) were below the tracks formed by the unusual light wave (polarization along the scanning direction) (Fig. 3, b for $\nu = 3$ kHz and $V_{wr} = 0.1$ mm/s).

In all the frequency modes, within the range 1–600 kHz, at the speeds from 33 μm/s to 20 mm/s the modified tracks reduced the refractive index as compared to the unmodified region, wherein the value of the refractive index varied within the range $|\Delta n| = 0.035–0.08$ (Fig. 3, c). The scanning direction ($+Z$ or $-Z$) did not substantially affect the value of $|\Delta n|$, i.e. no „quill writing“ effect was exhibited [46]. When writing with the beam with polarization perpendicular to the scanning direction V_{wr}, the values of contrast of the refractive index $|\Delta n|$ are slightly higher than for polarization parallel to V_{wr}. The track height for all the pairs ν and V_{wr}, which is determined by means of the optical microscope when analyzing the tracks via the polished butt end, was about 10 μm. Further on, in order to form the waveguides with the depressed cladding, we used the conditions $\nu = 90$ kHz, $V_{wr} = 3$ mm/s (when $E_p = 70–80$ nJ, $\tau_p = 175$ fs, polarization is perpendicular to the scanning direction), which resulted in quite high values of $|\Delta n|$ with the quite fast and well-controlled speed of translation of the sample in relation to the beam.

3. Waveguide formation

In order to create homogeneous tracks by the scanning beam of ultrashort pulses, it is necessary to maintain a constant number of the pulses N_p hitting the sample, which is determined by the relationship [17,45]:

$$N_p = \frac{D \cdot \nu}{V_{wr}}, \qquad (1)$$

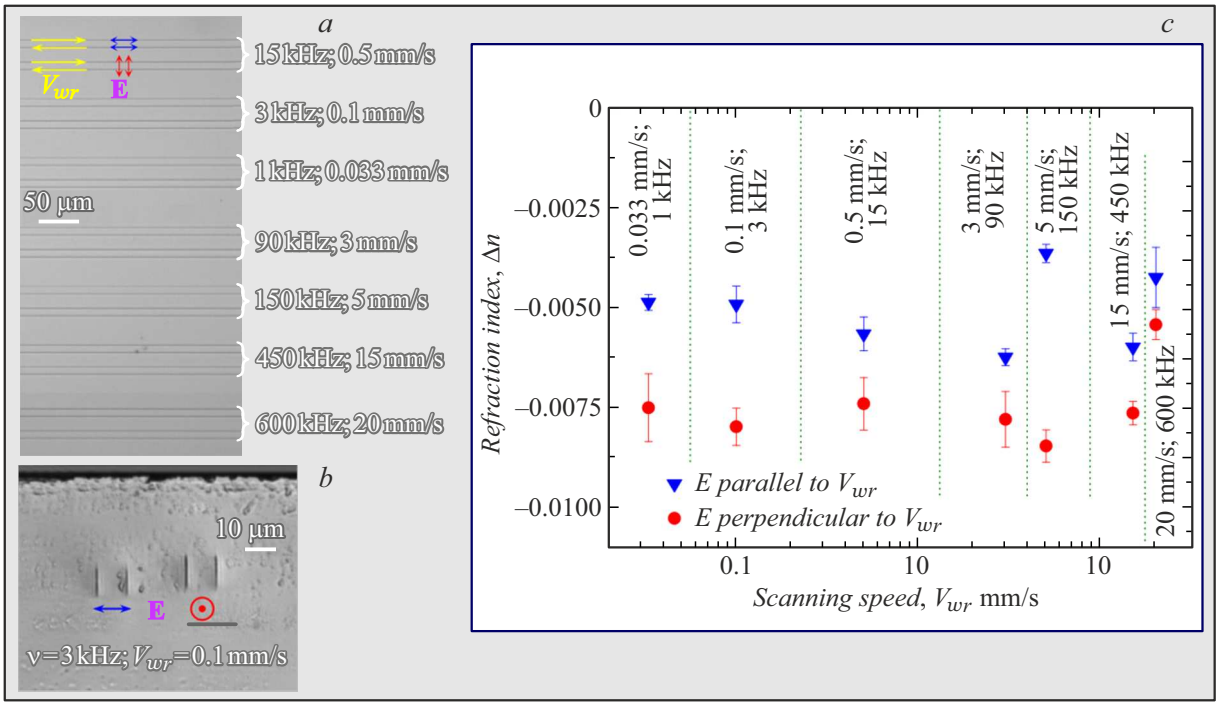

Figure 3. *a* — images obtained by means of the optical microscope for the tracks of the modified refractive index, which are written at the constant number of the laser pulses N_p, but at the various proportional values of the scanning speed V_{wr} and the femtosecond-pulse repetition rate ν (the plan view); *b* — the view from the butt end for the tracks formed when $\nu = 3$ kHz; $V_{wr} = 0.1$ mm/s; *c* — the diagram of contrast of the refractive index at the various pairs V_{wr} and ν (N_p = const).

where D is a laser spot diameter. Depending on the light-pulse repetition rate ν, various modes of femtosecond modification are possible, while the speed variation range is quite narrow — when V_{wr} is low multi-track waveguides will be written exceedingly long, and when V_{wr} is high, limitations will appear due to a translational system (vibrations, inhomogeneities of acceleration and deceleration when a scanning path is short). Therefore, in order to search for an optimal writing mode that makes it possible to create the smooth tracks with maximum contrast of the refractive index Δn, $LiNbO_3$ was modified with proportional variation of the pulse repetition rate ν and the beam scanning speed V_{wr}. With the constant value of the number of the pulses N_p, for each pair ν and V_{wr} we have formed the tracks at the constant energy $E_p = 80$ nJ within the femtosecond pulse for the two orthogonal polarizations of writing radiation (Fig. 3). The tracks written by the usual light wave (with polarization orthogonal to the scanning direction) were below the tracks formed by the unusual light wave (polarization along the scanning direction) (Fig. 3, *b* for $\nu = 3$ kHz and $V_{wr} = 0.1$ mm/s).

In all the frequency modes, within the range 1–600 kHz, at the speeds from 33 μm/s to 20 mm/s the modified tracks reduced the refractive index as compared to the unmodified region, wherein the value of the refractive index varied within the range $|\Delta n| = 0.035–0.08$ (Fig. 3, *c*). The scanning direction ($+Z$ or $-Z$) did not substantially affect the value of $|\Delta n|$, i.e. no „quill writing“ effect was exhibited [46]. When writing with the beam with polarization perpendicular to the scanning direction V_{wr}, the values of contrast of the refractive index $|\Delta n|$ are slightly higher than for polarization parallel to V_{wr}. The track height for all the pairs ν and V_{wr}, which is determined by means of the optical microscope when analyzing the tracks via the polished butt end, was about 10 μm. Further on, in order to form the waveguides with the depressed cladding, we used the conditions $\nu = 90$ kHz, $V_{wr} = 3$ mm/s (when $E_p = 70–80$ nJ, $\tau_p = 175$ fs, polarization is perpendicular to the scanning direction), which resulted in quite high values of $|\Delta n|$ with the quite fast and well-controlled speed of translation of the sample in relation to the beam.

4. Waveguide formation

The laser beam scanning for writing the depressed cladding was along the optical axis (along Z). The polarization direction was perpendicular to the scanning direction, i.e. along Y. The cladding of 32 tracks of the 10 μm height was written. The diagram of transverse arrangement of the tracks that form the waveguide is shown in Fig. 4, *a*, it is identical to architectures of waveguides from the studies [47,48]. An upper part and a lower part of the cladding consisted of 11 tracks, 5 tracks were on each side, the step between the adjacent tracks Δy was either 1 μm (Fig. 4, *b*) or 2 μm (Fig. 4, *c*). In the first case, the diameter

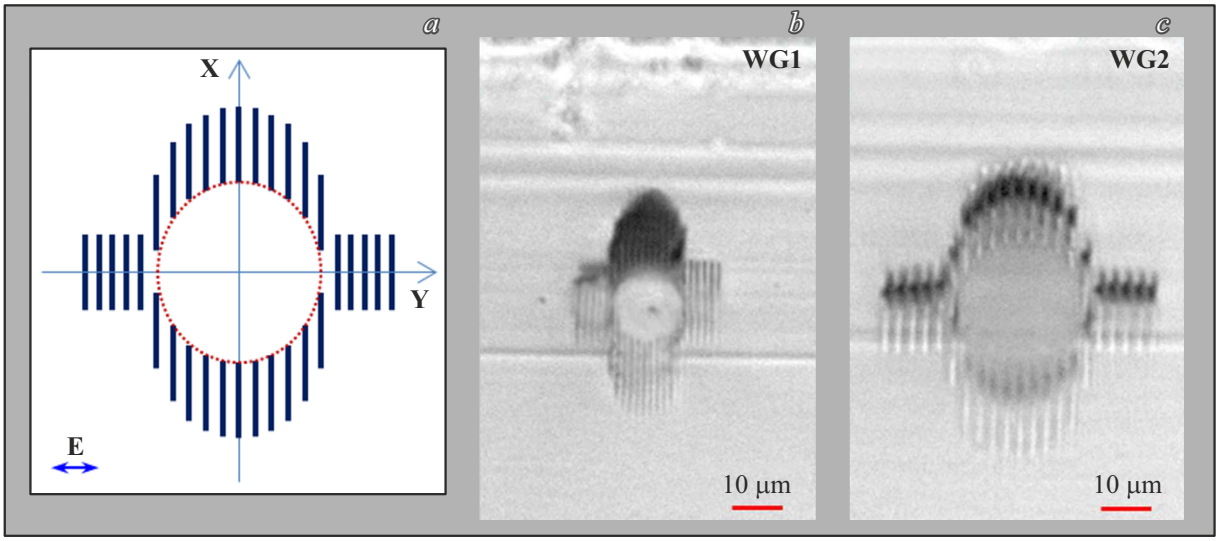

Figure 4. Planned profile of the waveguide structures (a). The profiles of the$LiNbO_3$-formed waveguides: a step between the adjacent tracks $\Delta y = 1$ (b) and $2\,\mu$m (c).

of the (unmodified) core was approximately $10\,\mu$m, while in the second case it was $20\,\mu$m. The tracks were written only when scanning along one direction $(+Z)$, while the sample was returned along the direction $-Z$ with the beam cut off. The burial depth of a waveguide center in relation to the surface, through which it was written, was $60\,\mu$m. The writing beam pulse energy was 70 nJ. It is clear in Fig. 4 that the formed waveguides correspond to the planned structure. The core is close to a round cross-section.

5. Coupling of the optical fiber and input of radiation into the formed waveguides

Prior to radiation input, the crystal butt ends were polished in order to exclude impact of possible defects. The crystal was fastened on the fixed table. On the one side (Fig. 5, a), we input a single-mode optical fiber of the SMF-28 type, which was connected to a source of optical radiation with the wavelength of $1.55\,\mu$m, a spectral band width of 10 kHz and power of 4 dBm. At the opposite side of the waveguide (Fig. 5, b), we input a similar optical fiber connected to an optical power meter. The two fibers and the waveguide were roughly aligned by means of visible radiation.

After rough alignment, each optical fiber was aligned in relation to the waveguide by an optical-signal maximum with an accuracy of up to $0.1\,\mu$m. Waveguide output intensity was profiled (Fig. 6) by means of an optical fiber coupling station equipped with linear piezopositioners with a 50 nm step. It was profiled by scanning the crystal butt end in a region of the waveguide output in a „snake“ algorithm with automatically recording each obtained values of transmitted optical power. Optical probes were flatly-

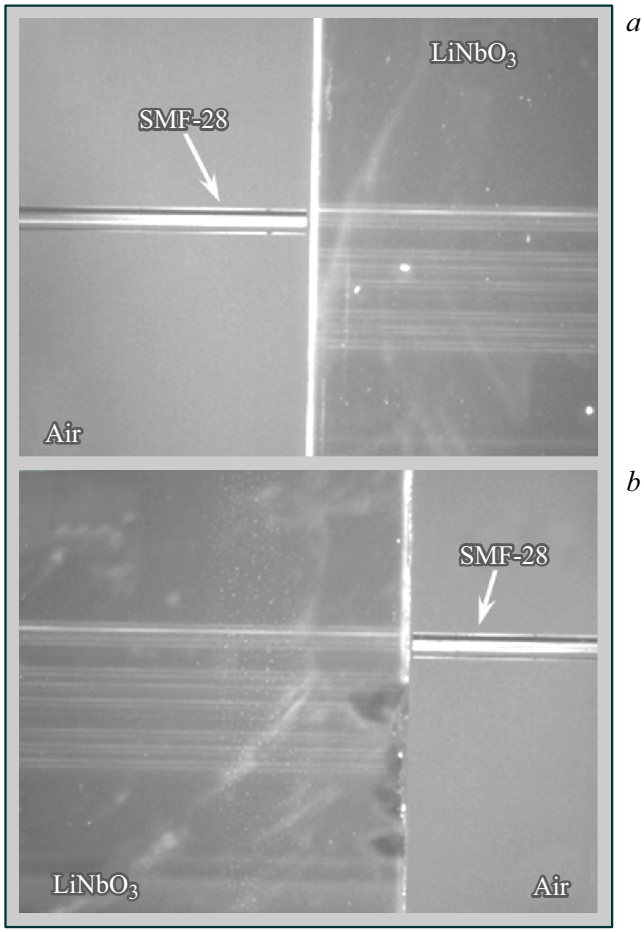

Figure 5. Photos shot from a vertical camera when aligning fiber lightguides with the crystal waveguides.

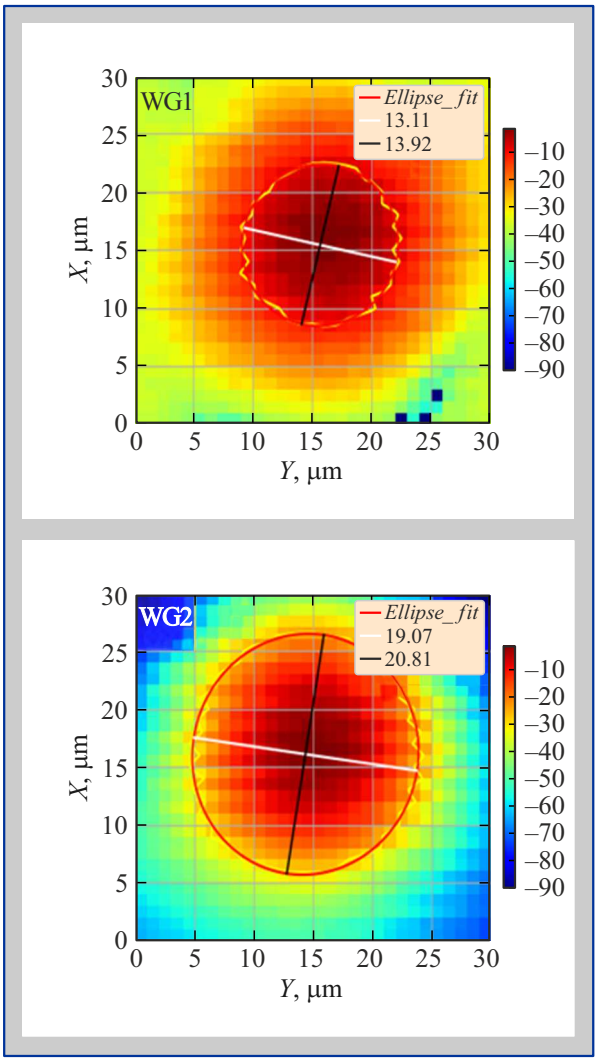

Figure 6. Dependence of an optical-signal level on shifts between the fiber lightguide and the waveguides WG1 (a) and WG2 (b).

cleaved single-mode optical fibers. We note that both the guided modes are characterized by a slightly elliptical profile. A length of a minor axis of the ellipse of the guided mode is 13.1 μm for the WG1 waveguide, so is 19.1 μm for the WG2 waveguide. For the WG1 waveguide, ellipticity of the guided mode ($k = B/A$, where B and A are semi-axes of the intensity profile ellipse) is $k_{M1} = 0.94$, while mode ellipticity for the WG2 waveguide is $k_{M2} = 0.91$, which quite well correlates with core ellipticities $k_{WG1} = 0.95$ and $k_{WG1} = 0.90$, which are evaluated by images from the optical microscope (Fig. 4, b, c).

Losses in a system that consists of the waveguides written by the femtosecond laser and the two optical fibers coupled to the waveguide butt ends (fiber-to-fiber) have been measured. The values obtained were at a level -4.5 dB (WG1) and -5.7 dB (WG2). With subtraction of radiation input/output losses that are at least 0.5 dB, it provides waveguide's linear losses of about 2 dB/cm (for WG1) and 2.5 dB/cm (WG2). The radiation input/output optical losses were estimated across a large scope of experiments previously done for coupling waveguides in lithium niobate and single-mode optical fibers. They were estimated by a method of subsequent chip shortening with plotting a dependence of fiber-to-fiber losses.

The studied sample has been taken to determine general losses in the system of the two optical fibers and the tubular waveguide written in lithium niobate. No separate experiments for determining input/output losses were done since the method is destructive. The provided estimation of the value of the optical losses is minimal, and for other cases the radiation input optical losses can be even higher, thereby meaning even lower values of losses for propagation of radiation in the formed waveguide with taking into account preservation of the value of the fiber-to-fiber optical losses.

The experimentally obtained values of the losses are quite low and correspond to photonic integrated circuit samples based on lithium niobate, whose waveguides are photolithographically formed. It indicates both attractiveness of the technology of direct laser writing of waveguides with reduced cladding contrast for $LiNbO_3$ as well as convenience of butt-end input/output of radiation by the single-mode optical fiber, thereby making this approach suitable for fast prototyping of the photonic integrated circuits and forming of structures with a complex topology, including a three-dimensional one.

Conclusion

Linearly-polarized femtosecond (175 fs) radiation with the wavelength of 1030 nm was used within the volume of the X-transect of the $LiNbO_3$ single crystal to implement writing of the tracks of the modified refractive index with various orientation of a polarization vector in relation to the optical axis of the crystal. It is shown that the tracks of the lower refractive index, which are formed by the usual light wave, are below the tracks written by the unusual light wave, which is related to the high refractive index for the usual wave in $LiNbO_3$.

When the pulse energies are within the range $E_p = 70-80$ nJ, the pulse repetition rate is $\nu = 90$ kHz and the laser beam sample scanning speed $V_{wr} = 3$ mm/s, the depressed-cladding waveguides of the length of 15 mm and the mode diameters 13 and 19 μm were formed along the direction of the optical axis (the Z axis). The optical fiber was input to the formed waveguides at the butt ends and guiding of radiation with the wavelength of 1.55 μm was demonstrated in the system of the two fiber lightguides and the tubular light guide in the $LiNbO_3$ volume with the least losses being about 2 dB/cm. The obtained results demonstrate that this approach based on integration of the waveguide formed by the femtosecond pulses and the commercial optical fiber is promising for various application of integral optics and engineering of photon integrated multi-element circuits.

Conflict of interest

The authors declare that they have no conflict of interest.

References

[1] K.K. Wong (ed.). *Properties of Lithium Niobate* (INSPEC, London, 2002)

[2] M.P. Sumets, V.A. Dybov, V.M. Ievlev. Inorg. Mater., **53** (13), 1361 (2017). DOI: 10.1134/S0020168517130015

[3] J.L. Jackel, C.E. Rice, J.J. Veselka. Appl. Phys. Lett., **41** (7), 607 (1982). DOI: 10.1063/1.93615

[4] P.G. Suchoski, T.K. Findakly, F.J. Leonberger. Opt. Lett., **13** (11), 1050 (1988). DOI: 10.1364/OL.13.001050

[5] K.R. Parameswaran, R.K. Route, J.R. Kurz, R.V. Roussev, M.M. Fejer, M. Fujimura. Opt. Lett., **27** (3), 179 (2002). DOI: 10.1364/OL.27.000179

[6] R.V. Schmidt, I.P. Kaminow. Appl. Phys. Lett., **25** (8), 458 (1974). DOI: 10.1063/1.1655547

[7] D. Hofmann, G. Schreiber, C. Haase, H. Herrmann, W. Grundkötter, R. Ricken, W. Sohler. Opt. Lett., **24** (13), 896 (1999). DOI: 10.1364/OL.24.000896

[8] E.L. Wooten, K.M. Kissa, A. Yi-Yan, E.J. Murphy, D.A. Lafaw, P.F. Hallemeier, D. Maack, D.V. Attanasio, D.J. Fritz, G.J. McBrien, D.E. Bossi. IEEE J. Sel. Top. Quant. Electron, **6** (1), 69 (2000). DOI: 10.1109/2944.826874

[9] L. Gui, B. Xu, T.C. Chong. IEEE Photon. Technol. Lett., **16** (5), 1337 (2004). DOI: 10.1109/LPT.2004.826112

[10] J. Burghoff, H. Hartung, S. Nolte, A. Tünnermann. Appl. Phys. A, **86**, 165 (2007). DOI: 10.1007/s00339-006-3750-6

[11] N.N. Skryabin, M.A. Bukharin, S.M. Kostritskii, Yu.N. Korkishko, V.A. Fedorov, D.V. Khudyakov. Radiopromyshlennost, **1**, 110 (2018).

[12] P. Wang, J. Qi, Z. Liu, Y. Liao, W. Chu, Y. Cheng. Sci. Rep., **7** (1), 41211 (2017). DOI: 10.1038/srep41211

[13] A.V. Sosunov, R.S. Ponomarev, S.S. Mushinsky, A.M. Minkin, A.B. Volyntsev. Ferroelectrics, **494** (1), 131 (2016). DOI: 10.1080/00150193.2016.1142333

[14] A.V. Sosunov, R.S. Ponomarev, S.S. Mushinsky, A.B. Volyntsev, A.A. Mololkin, V. Maléjacq. Crystallogr. Rep., **65** (5), 786 (2020). DOI: 10.1134/S1063774520050223

[15] G. Della Valle, R. Osellame, P. Laporta. J. Opt. A: Pure Appl. Opt., **11** (1), 013001 (2008). DOI: 10.1088/1464-4258/11/1/013001

[16] A. Okhrimchuk. *Femtosecond fabrication of waveguides in ion-doped laser crystals* (INTECH Open Access Publisher, 2010), p. 519−542. DOI: 10.5772/12885

[17] F. Chen, J.R. Vázquez de Aldana. Laser Photonics Rev., **8** (2), 251 (2014). DOI: 10.1002/lpor.201300025

[18] R. Osellame, H.J.W.M. Hoekstra, G. Cerullo, M. Pollnau. Laser Photonics Rev., **5** (3), 442 (2011). DOI: 10.1002/lpor.201000031

[19] T. Meany, M. Gräfe, R. Heilmann, A. Perez-Leija, S. Gross, M.J. Steel, M.J. Withford, A. Szameit. Laser Photonics Rev., **9** (4), 363 (2015). DOI: 10.1002/lpor.201500061

[20] B. Zhang, B. Xiong, Z. Li, L. Li, J. Lv, Q. Lu, L. Wang, F. Chen. Opt. Mater., **86**, 571 (2018). DOI: 10.1016/j.optmat.2018.11.001

[21] L. Li, W. Kong, F. Chen. Adv. Photonics, **4** (2), 024002 (2022). DOI: 10.1117/1.AP.4.2.024002

[22] M.R. Tejerina, D.A. Biasetti, G.A. Torchia. Opt. Mater., **47**, 34 (2015). DOI: 10.1016/j.optmat.2015.06.030

[23] R. Osellame, M. Lobino, N. Chiodo, M. Marangoni, G. Cerullo, R. Ramponi, H.T. Bookey, R.R. Thomson, N.D. Psaila, A.K. Kar. Appl. Phys. Lett., **90** (24), 241107 (2007). DOI: 10.1063/1.2748328

[24] R. Osellame, N. Chiodo, M. Lobino, M. Marangoni, G. Cerullo, R. Ramponi, H.T. Bookey, R.R. Thomson, N. Psaila, A.K. Kar. Proceed. SPIE, **6881**, 688112 (2008). DOI: 10.1117/12.763115

[25] A.G. Okhrimchuk, A.V. Shestakov, I. Khrushchev, J. Mitchell. Opt. Lett., **30** (17), 2248 (2005). DOI: 10.1364/OL.30.002248

[26] Ph.St.J. Russell. J. Lightwave Technol., **24** (12), 4729 (2006). DOI: 10.1109/JLT.2006.885258

[27] J. Hu, C.R. Menyuk. Adv. Opt. Photonics, **1** (1), 58 (2009). DOI: 10.1364/AOP.1.000058

[28] J. Lv, Y. Cheng, W. Yuan, X. Hao, F. Chen. Opt. Mater. Express, **5** (6), 1274 (2015). DOI: 10.1364/OME.5.001274

[29] R.R. Thomson, S. Campbell, I.J. Blewett, A.K. Kar, D.T. Reid. Appl. Phys. Lett., **88** (11), 111109 (2006). DOI: 10.1063/1.2186389

[30] J. Burghoff, S. Nolte, A. Tünnermann. Appl. Phys. A, **89**, 127 (2007). DOI: 10.1007/s00339-007-4152-0

[31] J. Burghoff, C. Grebing, S. Nolte, A. Tünnermann. Appl. Surf. Sci., **253** (19), 7899 (2007). DOI: 10.1016/j.apsusc.2007.02.148

[32] R. He, Q. An, Y. Jia, G.R. Castillo-Vega, J.R. Vázquez de Aldana, F. Chen. Opt. Mater. Express, **3** (9), 1378 (2013). DOI: 10.1364/OME.3.001378

[33] Q. Jia, P. Wang, Y. Liao, W. Chu, Z. Liu, Z. Wang, L. Qiao, Y. Cheng. Opt. Mater. Express, **6** (8), 2554 (2016). DOI: 10.1364/OME.6.002554

[34] S. Kroesen, K. Tekce, J. Imbrock, C. Denz. Appl. Phys. Lett., **107** (10), 101109 (2015). DOI: 10.1063/1.4930834

[35] H.-D. Nguyen, A. Ródenas, J.R. Vázquez de Aldana, G. Martín, J. Martínez, M. Aguiló, M.C. Pujol, F. Díaz. Opt. Express, **25** (4), 3722 (2017). DOI: 10.1364/OE.25.003722

[36] J. Lv, Y. Cheng, Q. Lu, J.R. Vázquez de Aldana, X. Hao, F. Chen. Opt. Mater., **57**, 169 (2016). DOI: 10.1016/j.optmat.2016.05.003

[37] T. Piromjitpong, M. Dubov, S. Boscolo. Appl. Phys. A, **125** (5), 302 (2019). DOI: 10.1007/s00339-019-2609-6

[38] S. Bhardwaj, K. Mittholiya, A. Bhatnagar, R. Bernard, J.A. Dharmadhikari, D. Mathur, A.K. Dharmadhikari. Appl. Opt., **56** (20), 5692 (2017). DOI: 10.1364/AO.56.005692

[39] C. Cai, J. Wang. Micromachines, **13** (4), 630 (2022). DOI: 10.3390/mi13040630

[40] R. Heilmann, C. Greganti, M. Gräfe, S. Nolte, P. Walther, A. Szameit. Appl. Opt., **57** (3), 377 (2018). DOI: 10.1364/AO.57.000377

[41] M. Macias-Montero, A. Dias, B. Sotillo, P. Moreno-Zárate, R. Ariza, P. Fernandez, J. Solis. J. Lightwave Technol., **38** (23), 6578 (2020). DOI: 10.1109/JLT.2020.3015013

[42] A. Barty, K.A. Nugent, D. Paganin, A. Roberts. Opt. Lett., **23** (11), 817 (1998). DOI: 10.1364/OL.23.000817

[43] D. Paganin, K.A. Nugent. Phys. Rev. Lett., **80** (12), 2586 (1998). DOI: 10.1103/PhysRevLett.80.2586

[44] M. Bukharin, D. Khudakov, S. Vartapetov. Phys. Procedia, **71**, 272 (2015). DOI: 10.1016/j.phpro.2015.08.300

[45] M.P. Smayev, P.I. Lazarenko, I.A. Budagovsky, A.O. Yakubov, V.N. Borisov, Y.V. Vorobyov, T.S. Kunkel, S.A. Kozyukhin. Opt. Laser Technol., **153**, 108212 (2022). DOI: 10.1016/j.optlastec.2022.108212
[46] P.G. Kazansky, W. Yang, E. Bricchi, J. Bovatsek, A. Arai, Y. Shimotsuma, K. Miura, K. Hirao. Appl. Phys. Lett., **90** (15), 151120 (2007). DOI: 10.1063/1.2722240
[47] A.G. Okhrimchuk, Yu.P. Yatsenko, M.P. Smayev, V.V. Koltashev, V.V. Dorofeev. Opt. Mater. Express, **8** (11), 3424 (2018). DOE: 10.1364/OME.8.003424
[48] A.G. Okhrimchuk, A.D. Pryamikov, A.V. Gladyshev, G.K. Alagashev, M.P. Smayev, V.V. Likhov, V.V. Dorofeev, S.E. Motorin, Y.P. Yatsenko. J. Lightwave Technol., **38** (6), 1492 (2020). DOE: 10.1109/JLT.2019.2954862

Translated by M.Shevelev